INTRODUCTION

According to accident statistics, [1,2] roof fall accidents occur quite frequently at the intersections of underground openings and account for up to 30% of the roof fall fatalities. But this figure will certainly go up considerably if roof falls not associated with any fatal accident are included in the analysis. Unfortunately, nonfatal roof falls are seldom documented.

In the underground coal mines, there are two types of entry intersections. One is the three-way (V type) and the other is the four-way (T type) intersections. A three-way intersection occurs whenever the mainline track haulageway turns at an angle into a section haulageway. The four-way intersections, by far the most common type in the U. S. underground coal mines, are formed by the intersections of two entries which are oriented perpendicular to each other or by the intersections of entries and crosscuts. However, crosscuts are frequently driven at an angle to the entry to facilitate machine movements. The four-way intersections formed by this method of crosscut development are angled.

At the intersection of two underground openings, the diagonal roof span is wider than the width of each individual opening. This is one of the major reasons why roof falls are more likely to occur at the intersections than in the entry between pillars. Consequently, special intersection support plans are usually employed (Figs. 1 and 2) for intersections. The most popular practices are to decrease roof bolt spacing 1 ft less than or to increase roof bolt length 1 to 2 ft longer than those employed in the entry between pillars.[3] The increase in bolt length or decrease in bolt spacing can be applied to all of the bolts in the intersection or employed only for the strategically located bolts depending on the individual mine practices. These rather generalized practices seem to be adequate for some areas but in many cases are inadequate for others. Occasionally, the neighboring two lines of chain pillars are staggered such that the crosscuts in one row of chain pillars face the centers of the chain pillars in the neighboring rows. This layout forms T-type three-way intersections which are also inadequate for most weak roofs.[3,4]

A study was therefore initiated to develop special techniques for intersection supports. The first phase of the study was the analysis of the stress fields for the underground entry intersections. A three-dimensional stress analysis was necessary for this purpose. Unfortunately, the three-dimensional problems of complicated boundary conditions are beyond the existing analytical methods. The three-dimensional finite element method (FEM) was therefore employed in this study. In the analysis, square pillars of 40 feet wide and an entry height of 8 feet were assumed while entry widths varied at 14, 20, and 26 feet. This model was selected to simulate the mine where roof fall data were collected. The second phase of the study was the collection of field data. The sizes of the roof falls including heights, lengths and widths were collected and analyzed. In the third phase study, the results of the first and second phases were compared and discussed. The analysis of field data

revealed an arching zone within which roof falls occurred. The arching zone above an entry obtained empirically was compared with the calculated stress contours. Assuming that the bolts must be anchored in the rock strata outside the arching zone, the preferable systems of bolting were proposed. Also the amount of pretension required to inhibit sliding between layers was discussed.

FINITE ELEMENT MODEL ANALYSIS

The Model

The problem to be considered here is the analysis of a four-way entry intersection excavated in the elastic, homogeneous and isotropic materials subjected to a vertical load equal to the overburden weight. A plane view of the four-way entry intersection is shown in Fig. 3. In the analysis, an entry height of 8 feet was assumed while entry widths varied at 14, 20, and 26 ft. Pillars which consist of coal were assumed to be square and 40 feet wide. Because of geometrical symmetry only the region, ABCD, was considered.

The idealized structural model of the region, ABCD, used in the finite element method is shown in Fig. 4. The model consists of rock and coal. The coal seam of eight feet thick is 592 ft. below surface. The material properties used in the calculation are shown in Table 1. The model was divided into 521 three-dimensional hexahedrom elements each of which has eight nodes and 24 translational degrees of freedom. The model thus contained a total of 729 nodal points and 2187 degrees of freedom. Considering the symmetry of the structure, boundary conditions were assumed as follows:

1. On the vertical planes at the boundary, the displacements normal to each plane were constrained while external forces parallel to each plane were zero.

2. On the surface, neither displacement constraint nor external force existed.

3. On the bottom, the displacements in three-directions were constrained.

The computer program "NASTRAN" developed by NASA was used throughout the analysis.[5]

Results

The stresses, σ_x, σ_y, σ_z, and displacements d_s, d_y, d_z were obtained for each of the 521 elements. Since it is rather cumbersome to present all of the data, only those relevant to the subsequent analysis will be discussed here.

The vertical stress, σ_z, on the horizontal plane at midheight of the coal seam is shown in Fig. 5. The results indicate that for the 20 ft. entry intersection, the maximum vertical stress, σ_{max}, occurs at the corners of the

pillar while the minimum stress occurs at the center of the pillar. The results for the 14 and 26 ft. entry intersections show similar trends except the overall stress level is lower for the 14 ft. entry intersection while higher for the 26 ft. entry intersection. Regardless of entry widths, the maximum vertical stress is related to the average stress in the pillar by

$$\sigma_{max} = 1.27\ \sigma_{ave}. \tag{1}$$

The average pillar stress is defined as

$$\text{ave} = \left(\frac{W_e + W_p}{W_p}\right)^2 \sigma_o \tag{2}$$

where σ_o is the overburden stress, and W_e and W_p are the widths of entry and pillar, respectively.

Fig. 6 shows the vertical displacement, d, at the roofline of the 20 ft. entry intersection. The maximum vertical displacement (d_{max}) which occurs at the center of the intersection is again related to the average pillar displacement by a constant (Fig. 7).

$$d_{max} = 1.47\ d_o \tag{3}$$

and

$$d_o = \frac{H_e}{E_c}\ \sigma_{ave} \tag{4}$$

where H_e is the entry height and E_c is the Young's Modulus of the coal pillar. The difference between the maximum displacement at the center of the intersection and the minimum displacement at the center of the pillar decreases as it moves upward into the roof. The difference becomes negligible at a height approximately one entry width above the roofline.

The vertical stress at the roofline is more complicated (Fig. 8). Small tensile stress occurs at the center of the intersection and along the centerline of the entry whereas compressive stress increases toward the pillar and reaches the maximum value near the ribs. The areas where tensile stress occurs increase with the entry widths (Fig. 9). It is restricted to a small circular area at the center of the 14 ft. entry intersection but expands along the axes of the entries as the entry width increases. A high stress concentration occurs at the corners of the pillar (Fig. 10), the maximum value of which is found at the midheight of the pillar. A highly destressed zone resembling an arch forms above the intersection.

The horizontal stress contours at the roofline are much more complicated. The maximum tensile stress appears near the corner B (Fig. 11). A secondary maximum tensile stress occurs at the center of the intersection. The maximum compressive horizontal stress develops near the pillar ribs on the crossection AB. However, the horizontal stress at the roofline is highly dependent on the Poisson's ratio of the roof rock. A larger Poisson's ratio which produces a larger confining pressure caused the tensile horizontal stress to

restrict to a smaller area. As the Poisson's ratio decreases, the tensile stress region increases (Fig. 12).

COLLECTION AND ANALYSIS OF FIELD DATA

The field data of roof falls at the entry intersections were collected in an underground coal mine 592 ft. below surface. The coal seam was the Pittsburgh seam with an average thickness of 8 ft. The entry width was 20 ft. A total of 22 roof falls occurred and records were kept during the data collection period. Since most roof falls assumed dome shapes with irregular bottoms, the measured parameters are the maximum (D_{max}) and the minimum (D_{min}) dimensions of the bottom, and the height of the roof falls. The maximum and the minimum dimensions were measured at the roof line while the heights were measured from the roofline to the highest points of the falls which were generally at the centers of the falls.

The maximum bottom dimension of the fall ranges from 11 to 55 ft with an average value of 28.27 ft. The minimum bottom dimension ranges from 9 to 30 ft with an average value of 18.9 ft, and the height ranges from 4 to 11 ft with an average value of 8.45 ft (Fig. 13). If a nominal bottom dimension (D_n) is defined as:

$$D_n = \sqrt{D_{max} \cdot D_{min}} \tag{5}$$

then the nominal dimension is related to the average height of the fall by the following equation (Fig. 14)

$$H_f = 0.37\ D_n \tag{6}$$

Since the average nominal dimension for all of the roof falls was 22.65 ft. the average height (H_f) of the falls based on Eq. 6 was 8.38 ft. Comparing the values of these two parameters (ie, D_n and H_f) with the stress distribution calculated for the 20 ft entry intersection, it was found that the vertical stress contour line of $\sigma_z = 0.1\sigma_o$ conforms to the arch shape formed by the average roof fall dimensions of D_n = 22.65 ft and H_f = 8.38 ft (Fig. 15). Using the criterion that the contour line, $\sigma_z = 0.1\sigma_o$ defines the boundaries of the arch zone above the intersection that has more or less lossened up and requires supports, the widths and heights of the arch zones above the intersections of various entry widths can be determined as shown in Fig. 15.

PROPOSED ROOF BOLTING SYSTEMS

Suspension Method

If the rock strata within the arch zones discussed previously break and require immediate support, the roof bolt patterns should be designed to carry the rock weight in this region. The idea is to suspend the broken rock to the overlying intact main roof. Fig. 16 shows the contour lines of the upper boundary of the arch zone above the roofline while Fig. 17 indicates the proposed bolt length distribution patterns for the 20 ft wide entry, assuming that at least one extra foot of the bolts must be anchored at the strata outside the

arch zone. Region I which covers the center of the intersection requires a bolt length equal to or longer than one half of the entry width while those near the corners (Region II) require a bolt length only one half of those in Region I. The carrying weight per unit area in Region I is $1/2\rho_R$ g W_e and that in Region II is $1/4\rho_R$ g W_e, where ρ_R g is the unit weight of the strata.

Similar criteria can be applied to the intersections of various entry widths, including the 14-, and 26-ft entry intersections investigated in this report.

Friction Reinforcement Method

If there are thinly laminated strata in the immediate roof, roof bolting patterns should also be designed to strengthen these strata. This can be achieved by tightening them together to become a combined thick beam. A thicker beam deflects or sags less than a thinner one. The principle behind the beam building is to increase the frictional shear resistance between the interstrata beddings which reduces or prohibits interstrata sliding.

The shear resistance, S_r, required to prevent sliding between strata may be calculated by the following equations:

$$\text{if } \sigma_z > 0,\ S_r = \tau_r - \mu\sigma_z - \tau_o \qquad (7)$$

$$\text{if } \sigma_z < 0,\ S_r = \tau_r - \tau_o$$

where $\tau_r = \sqrt{\tau_{xz}^2 + \tau_{yz}^2}$, μ is the coefficient of friction and τ_o is the cohesive shear strength between strata. If the assumptions that $\mu = 1$ and $\tau_o = 0$ are made for Eq. 7, the shear resistances required to prevent slidings between strata are shown in Figs. 18 and 19. The most critical area where the required shear resistance reaches the maximum value is located in a horizontal plane approximately 3 ft above the roofline (Fig. 18). The maximum required shear resistance on the horizontal plane is found near the corners. It decreases toward the center and the corners of the intersection.

The required shear resistance varies with the widths of entry, coefficients of friction and cohesive shear strengths. The effects of these parameters are shown in Figs. 20 and 21. For a constant coefficient of friction, the required shear resistance decreases either with increases in cohesive shear strength of the interstrata beddings or with decreases in $W_e/(W_p + W_e)$ and τ_o/σ_o, the required shear resistance increases with increases in coefficient of friction (Fig. 20).

The required bolt lengths for frictional reinforcement can be determined by defining the region in which $S_r \geq 0$. The condition $S_r \geq 0$ simply means that there is a need of frictional reinforcement to provide shear resistance. Therefore, the required bolt lengths are the heights of the regions above the roofline where $S_r \geq 0$. Based on this criterion the bolt lengths for various combinations of μ, $W_e/(W_e + W_o)$ and τ_o/σ_o are shown in Fig. 21. For a constant μ, the required bolt lengths increase with increases in the ratios of $W_e/(W_e + W_p)$ and τ_o/σ_o. Similarly, for a constant value of $W_e/(W_e + W_p)$

and τ_o/σ_o, the required bolt lengths decrease with increases in μ. The required bolt length for the frictional reinforcement can be either longer or shorter than that required for the suspension method depending on the various combinations of τ_o/σ_o, $W_e/(W_e + W_p)$, and μ (Fig. 17).

Comparison Between the Two Methods of Reinforcement

The required bolt lengths in both methods are proportional to the entry widths. But in the suspension method the required anchorage capacity or strength and length of the bolt neither vary with the coefficient of friction between strata, nor the cohesive shear strength whereas in the friction reinforcement method they are highly dependent on these two parameters. Therefore in designing an optimum roof bolting pattern for an underground four-way entry intersection, the required anchorage capacities or strengths and lengths of the bolts shall be calculated for both methods. A choice between the two methods can then be made based on the available anchorage capacity, bolt length, strata conditons and other requirements.

To illustrate the design procedures, an example is shown in Table 2 for a 20 ft. entry intersection. Clearly the bolt length required for the friction method is much shorter than the suspension method but the bolt strength or anchorage capacity required for the friction method is larger than the suspension method when $\tau_o/\sigma_o \leq 0.02$. If there are numerous thinly laminated strata in the immediate roof, the minimum length and strength of the roof bolts should meet the requirements stated in the friction reinforcement method. Conversely if the immediate roof is fairly thick but breaks easily without supports, the minimum bolt length and strength (or anchorage capacity) should be selected based on the suspension method. However, in most underground coal mines the roof conditions do not provide a clearcut dividing line for either the suspension or the friction method. Under such conditions, the most reliable method is probably to deisgn for the most severe case required for both the suspension and the friction reinforcement.

CONCLUSIONS

1. The calculated results indicate that an arching zone is formed above a four-way intersection and a region of vertical tensile stress is developed over a short distance into the roof.

2. The analysis of field data combined with the calculated result shows that roof falls occur within the region where $\sigma_z \geq 0.10\sigma_o$.

3. Suspension and reinforcement methods of roof supports were studied. Preferable bolting systems for both methods were proposed in the paper.

REFERENCES

1. Dougherty, J. J., A Study of Fatal Roof Fall Accidents in Bituminous Coal Mines. M. S. E. M. Thesis, West Virginia University, Morgantown, WV, 1971, 77 pps.

2. Van Besien, A. C., "Analysis of Roof Fall Accident Statistics and Its Application to Roof Control Research." Paper presented at the AIME Annual Meeting, Chicago, Ill., Feb. 25 - March 1, 1973, Preprint No. 73-F-71, 11 pps.

3. Stahl, R. W., "Survey of Practices in Controlling Roof at Intersections and Juctions in Underground Coal Mines." U. S. Bureau of Mines, IC 8113, 1962, 13 pps.

4. Peng, S. S., "How Five Different Mines Apply Shortwall Methods to Mine Coal." Coal Age, March, 1976, p. 82-88.

5. McCormick, C. W. (Ed.) The NASTRAN User's Manual (Level 15.0), National Aeronautics and Space Administration, Washington, D. C., 1973.

TABLE 1. Properties of Rock and Coal

	Young's modulus kP/ft^2	Poisson's ratio	Specific Gravity
Rock	1.83×10^5	0.25	2.5
Coal	0.55×10^5	0.30	1.3

TABLE 2. Required Strength and Length of a Bolt for 20' Entry Intersection

Assumed Values in the Calculation

We = 20'

Wp = 40'

μ = 1.0

$\rho_R g$ = 150 lbs/ft^3

σ_o = 89000 lbs/ft^2

bolt pattern: 4' x 4'

	Suspension Method	Friction Method		
τ_o/σ_o	Any Value	0	0.02	0.04
Bolt length (ft.)	10'	5.7	4.9	3.7
Bolt Strength*(lb) or Anchorage Capacity	24,000	74,000	46,000	17,000

* Shear strength for a resin bolt and tensile strength for the others.

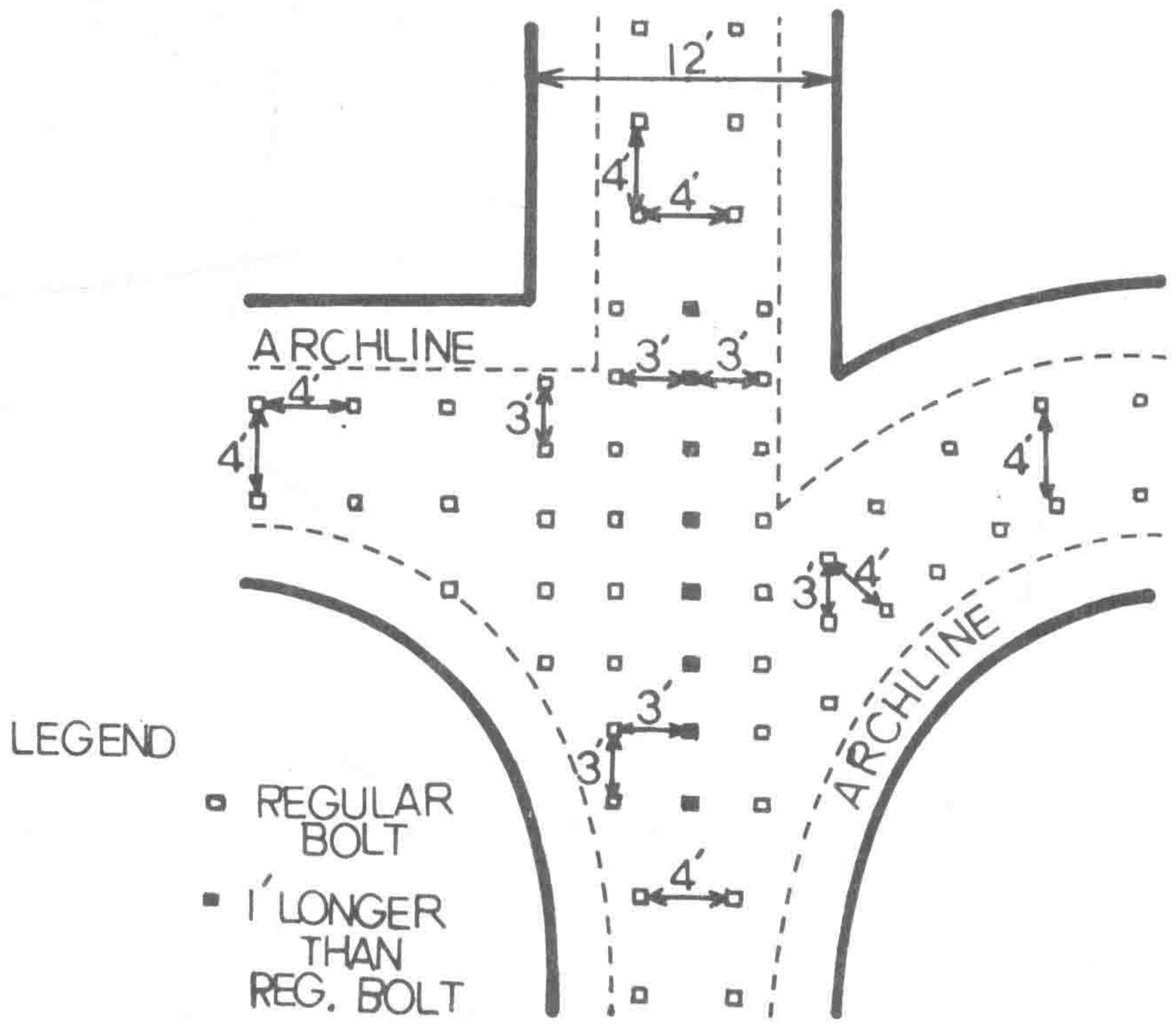

ROOF SECTION	
SANDSTONE	
SHALE	5' — 6'
BONY AND BANDS	12"
COAL	8" — 12"
DRAWROCK	8" — 12"
ROOF COAL	8" — 12"
PITTSBURGH COALBED	84"

Fig. 1 Special Intersection Support for Boring Type Miner

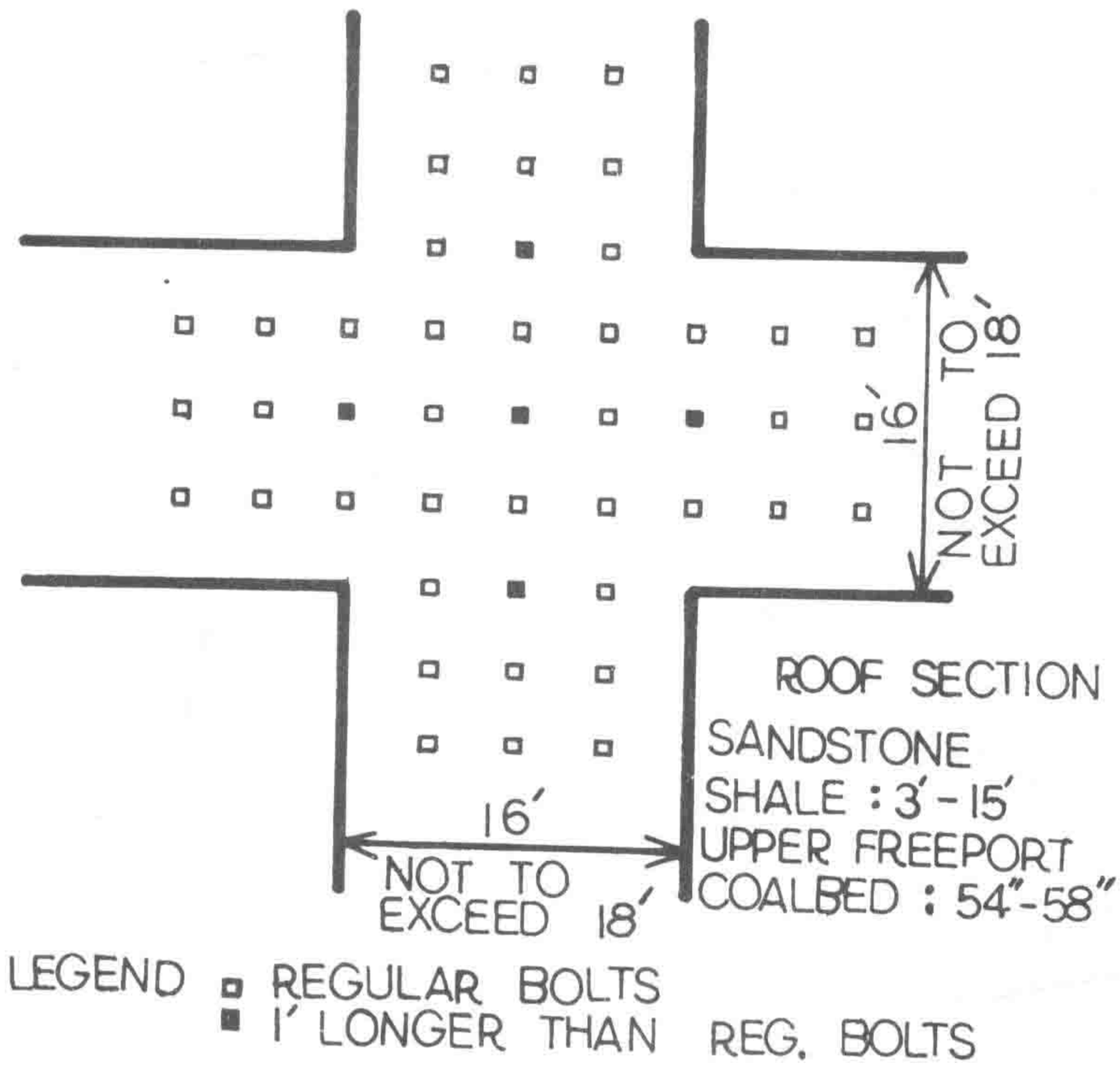

Fig. 2 Special Intersection Support for Ripper and Boring Type Miners

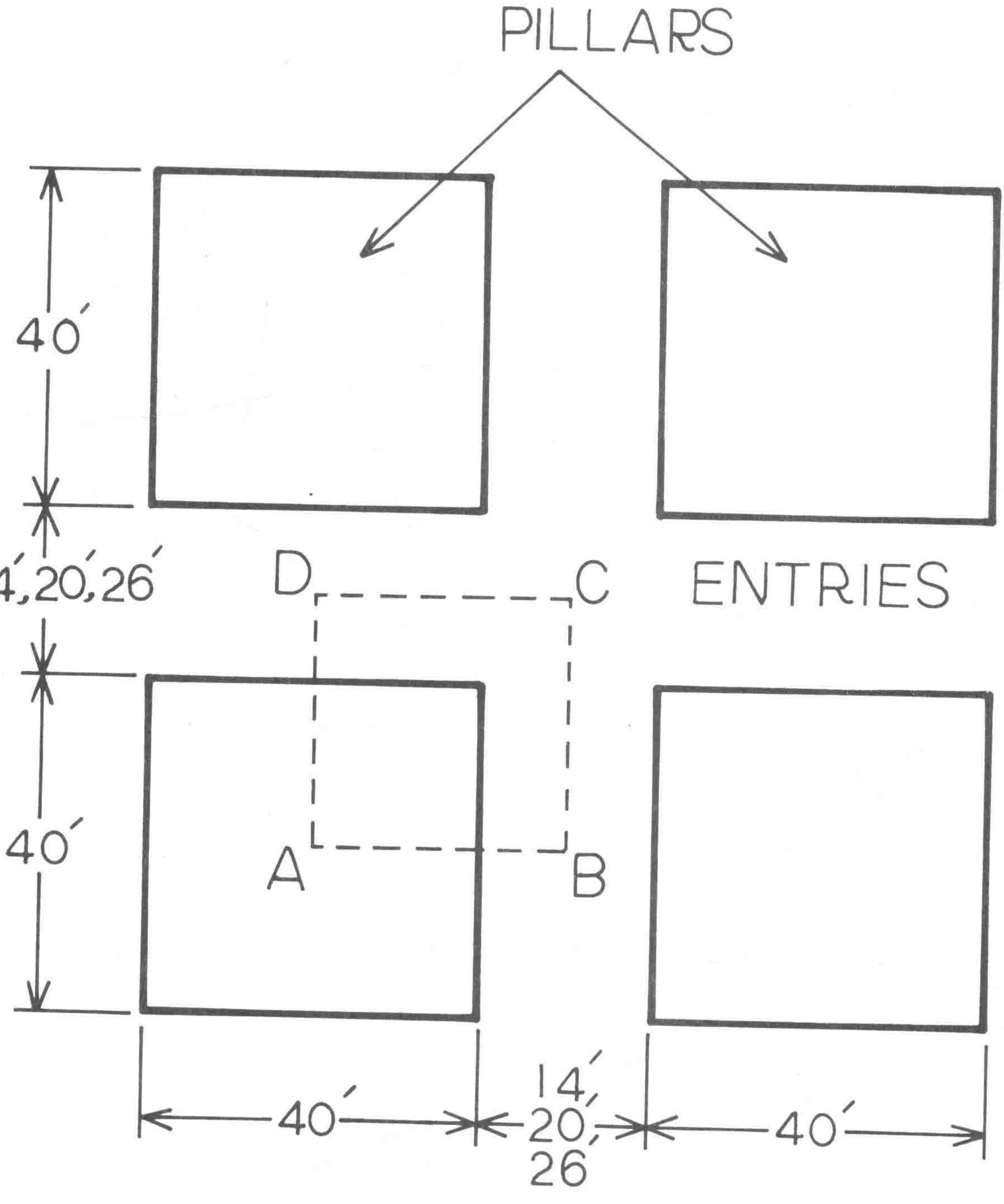

Fig. 3 Plan View of the 4-Way Intersection

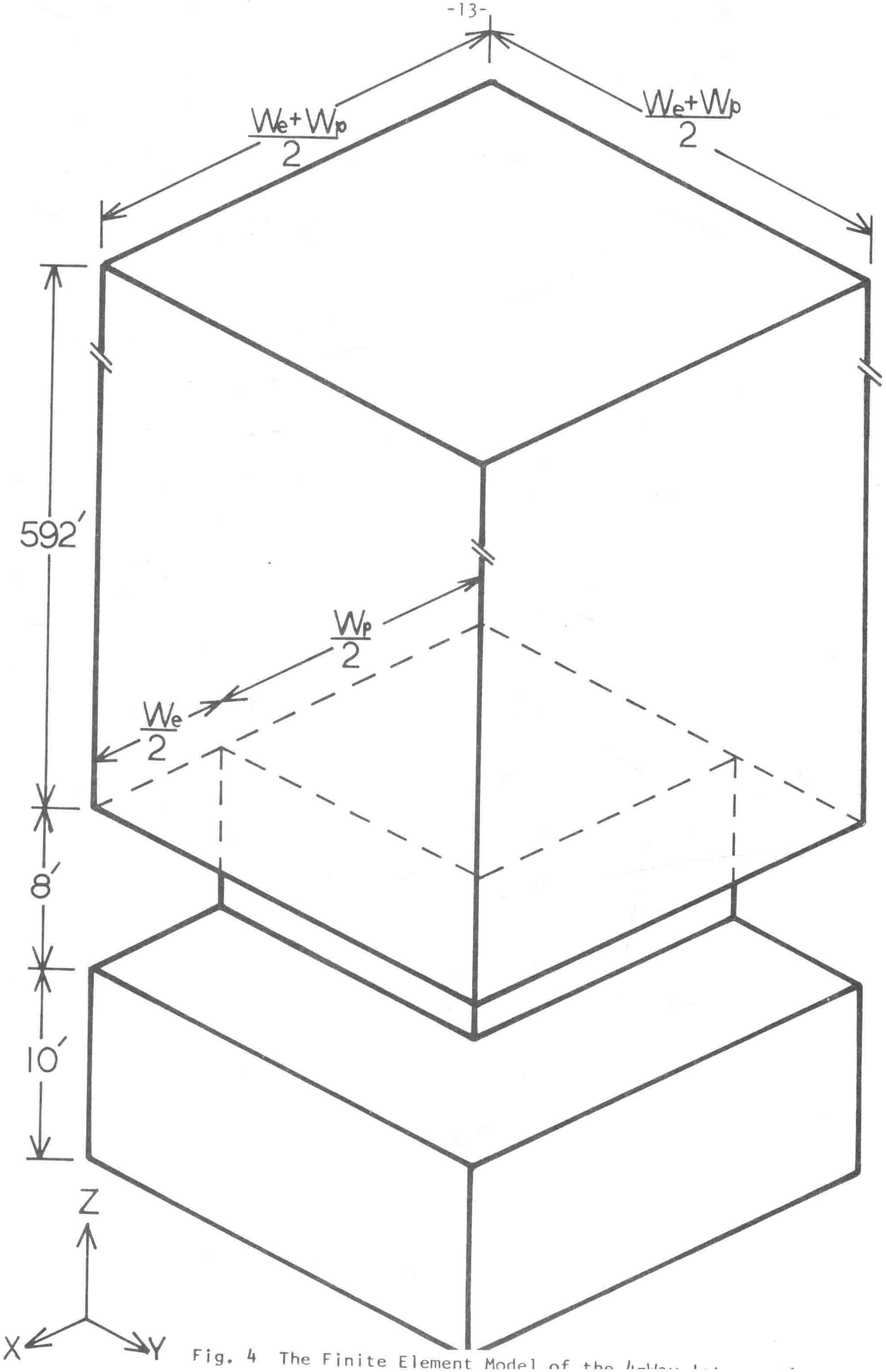

Fig. 4 The Finite Element Model of the 4-Way Interchange

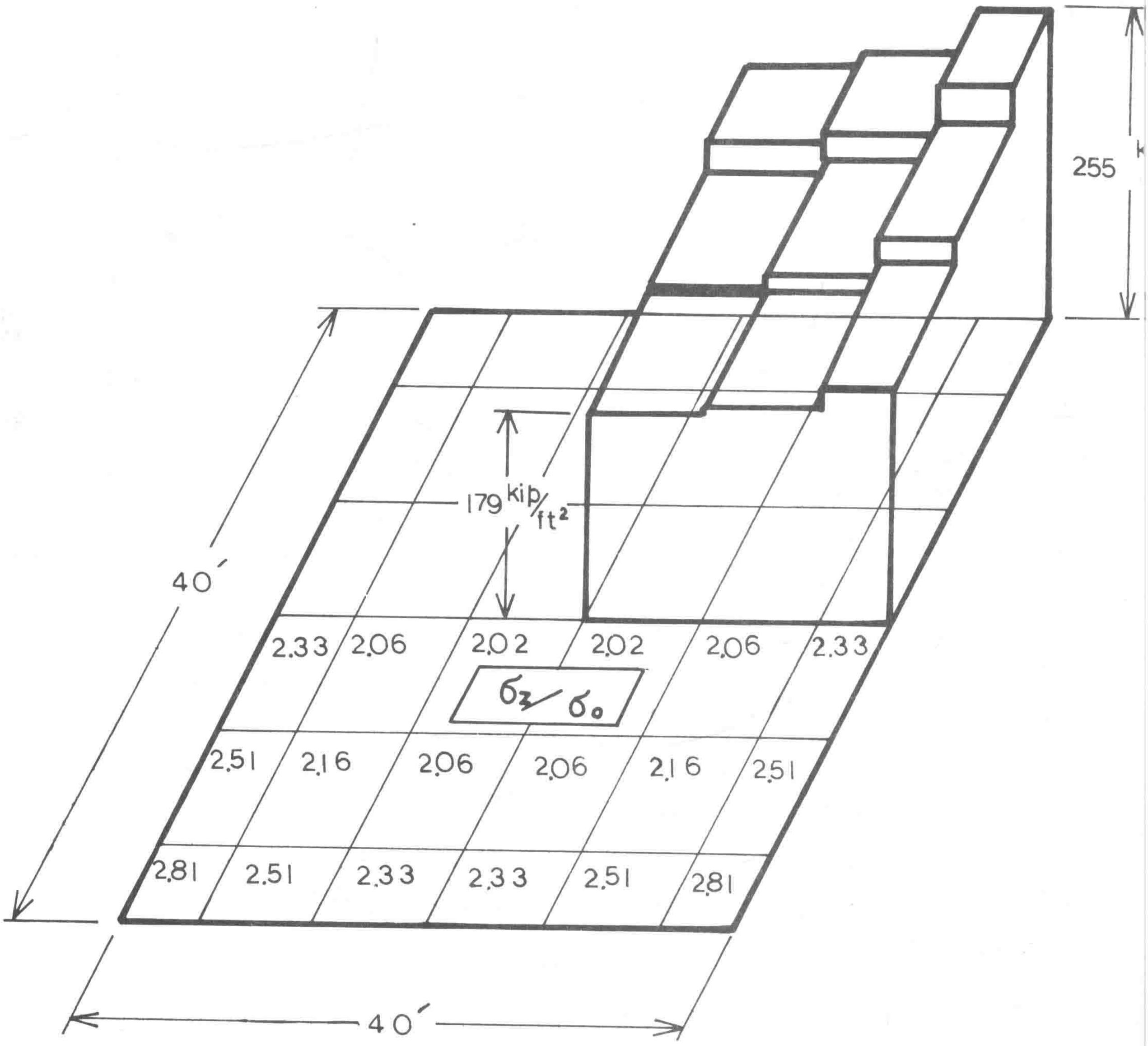

Fig. 5 Vertical Stress Distribution at Midheight of the Coal Seam

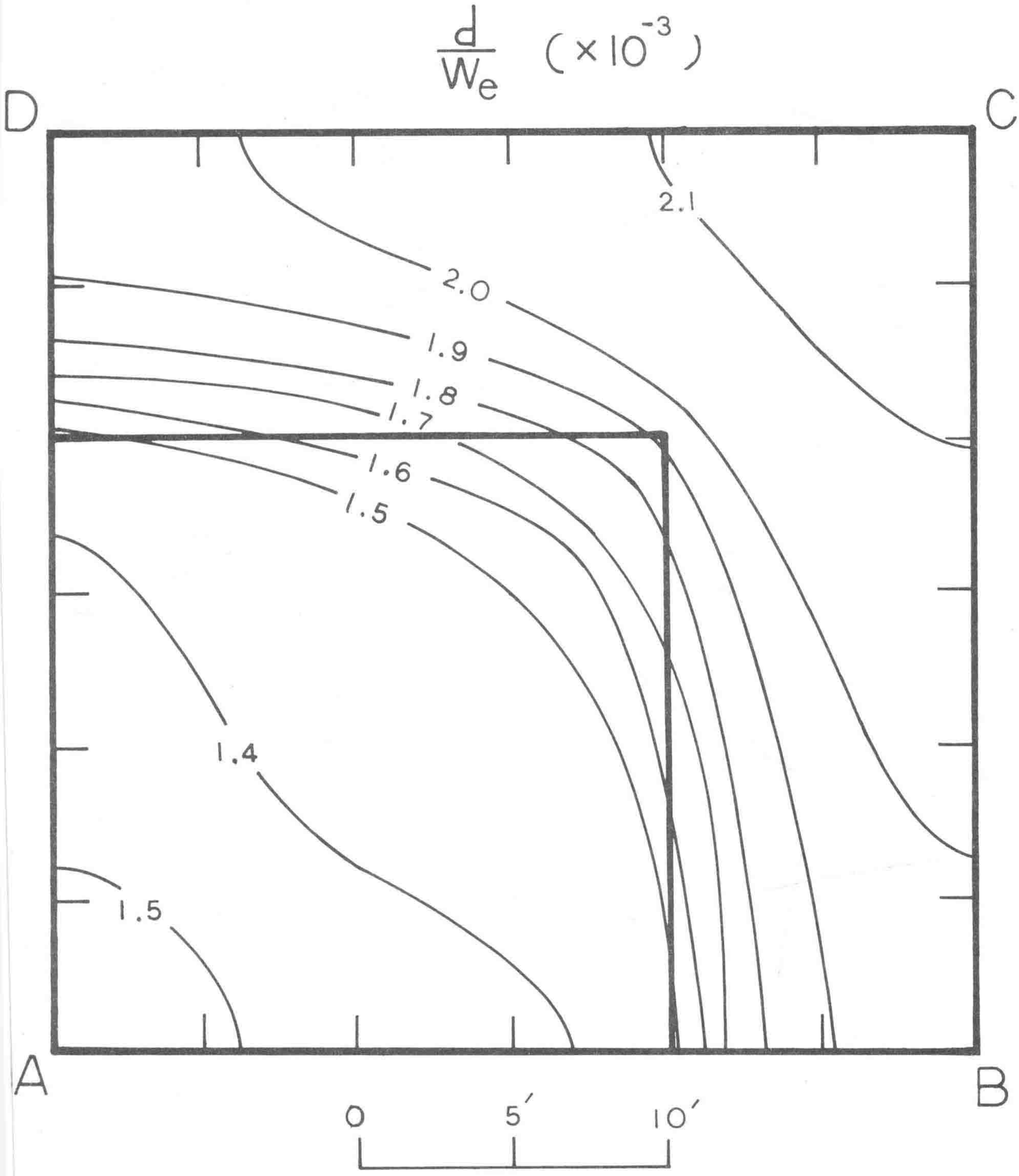

Fig. 6 Vertical Displacement at the Roof Plane

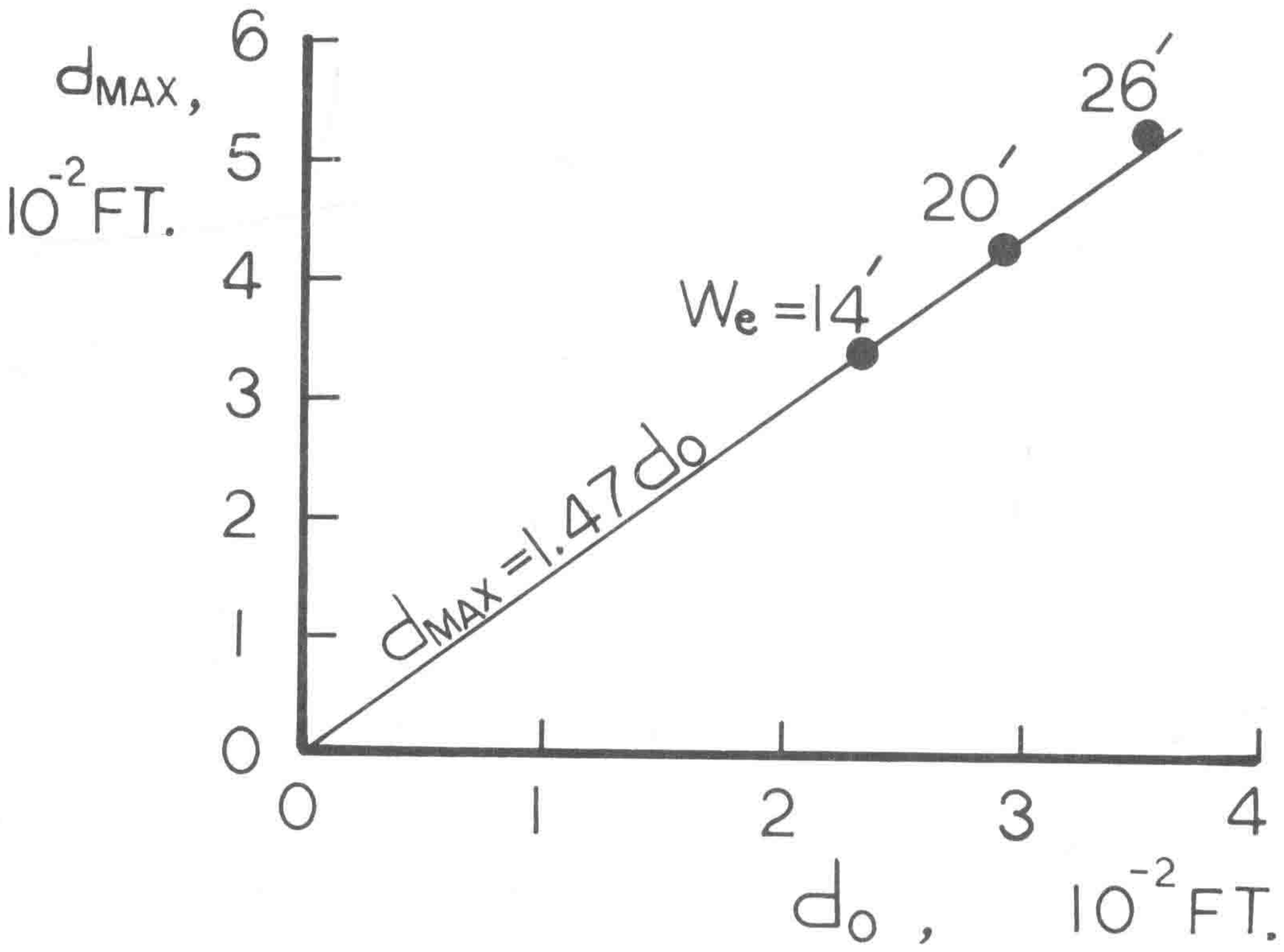

Fig. 7 Maximum Vertical Displacement at the Roof Plane

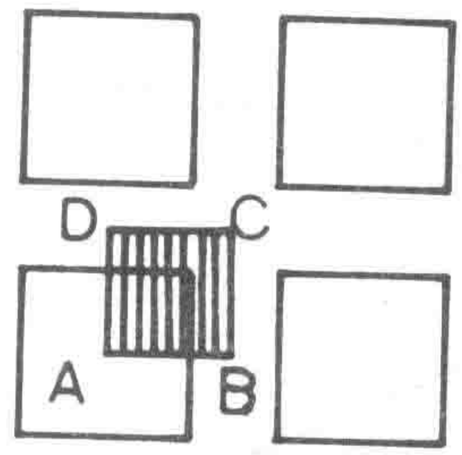

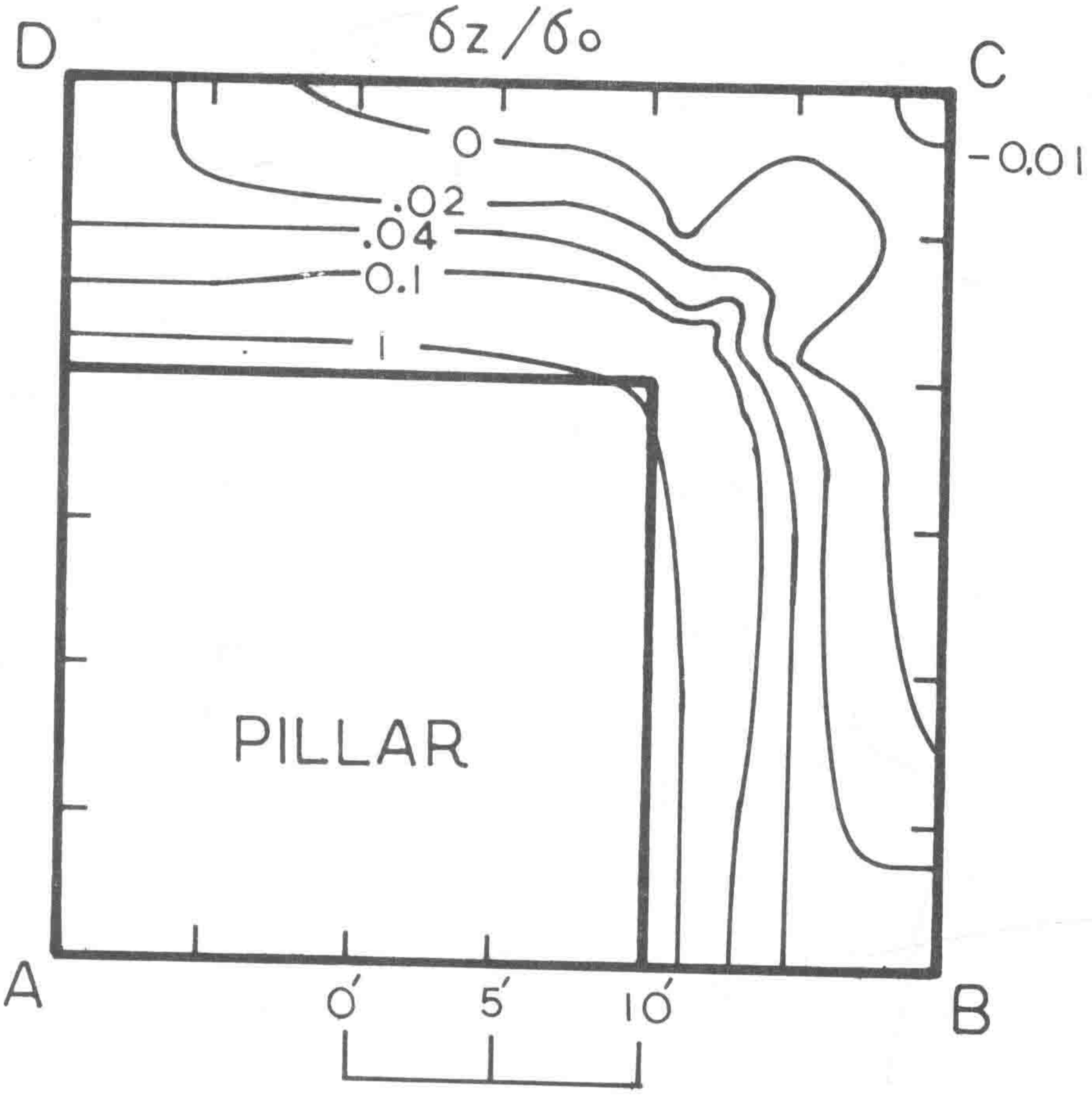

Fig. 8 Vertical Stress Contour at 1 Ft. Above the Roof Plane - 20 Ft. Entry Intersection

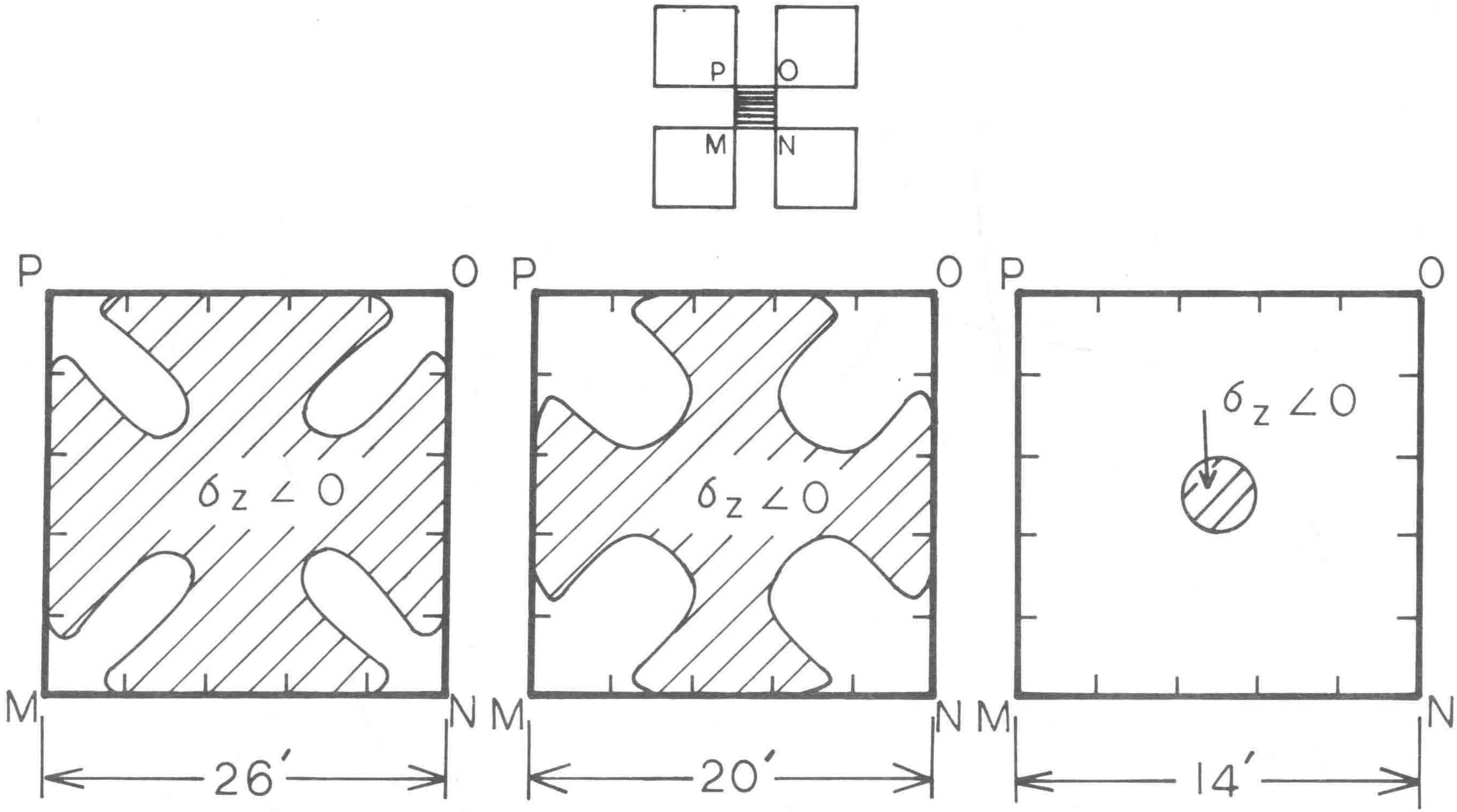

Fig. 9 Tensile Stress Zone at 1 Ft. Above the Roof Plane - 20 Ft. Entry Intersection

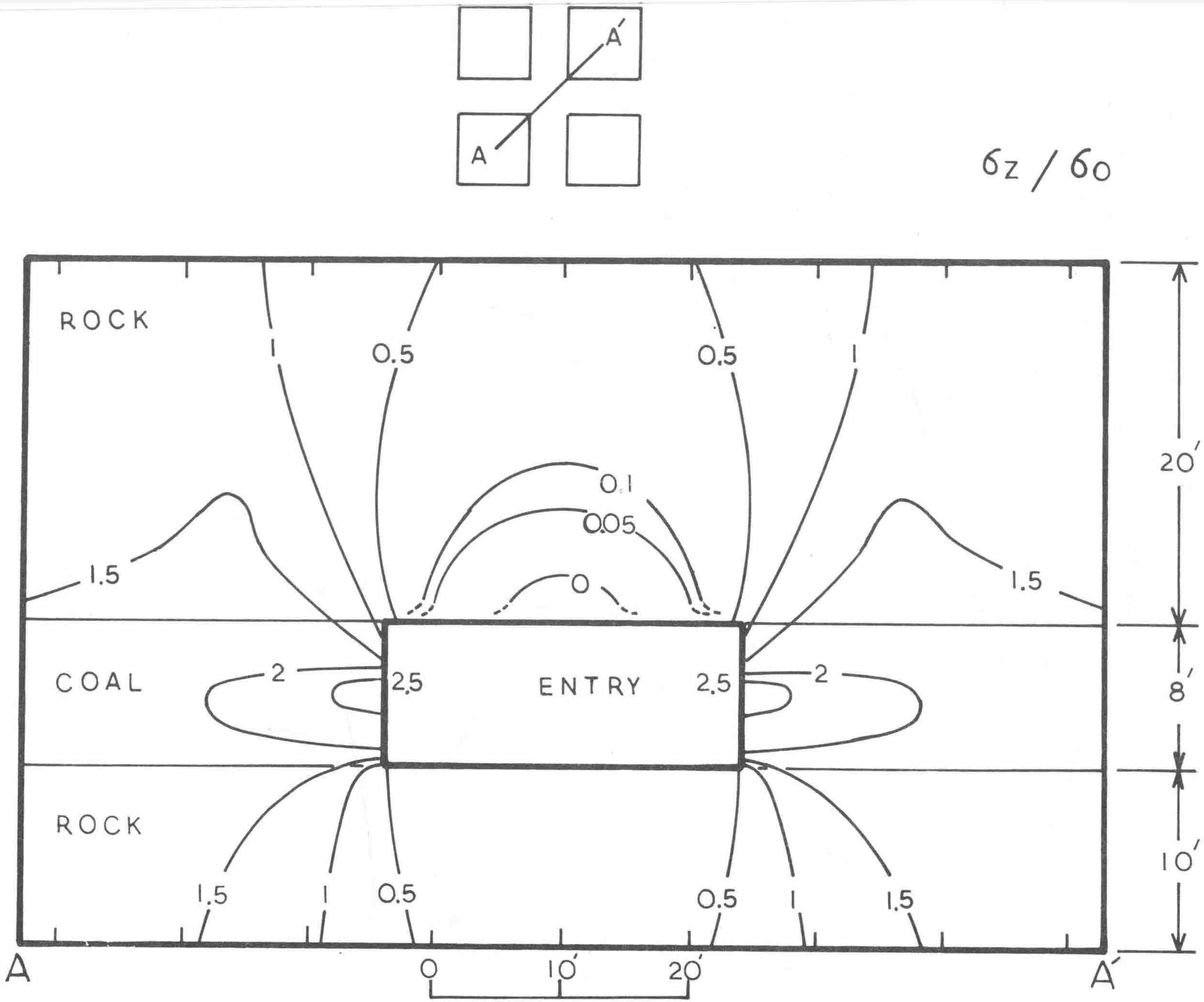

Fig. 10 Vertical Stress Controus at the A-A' Cross-Section - 20 Ft. Entry Intersection

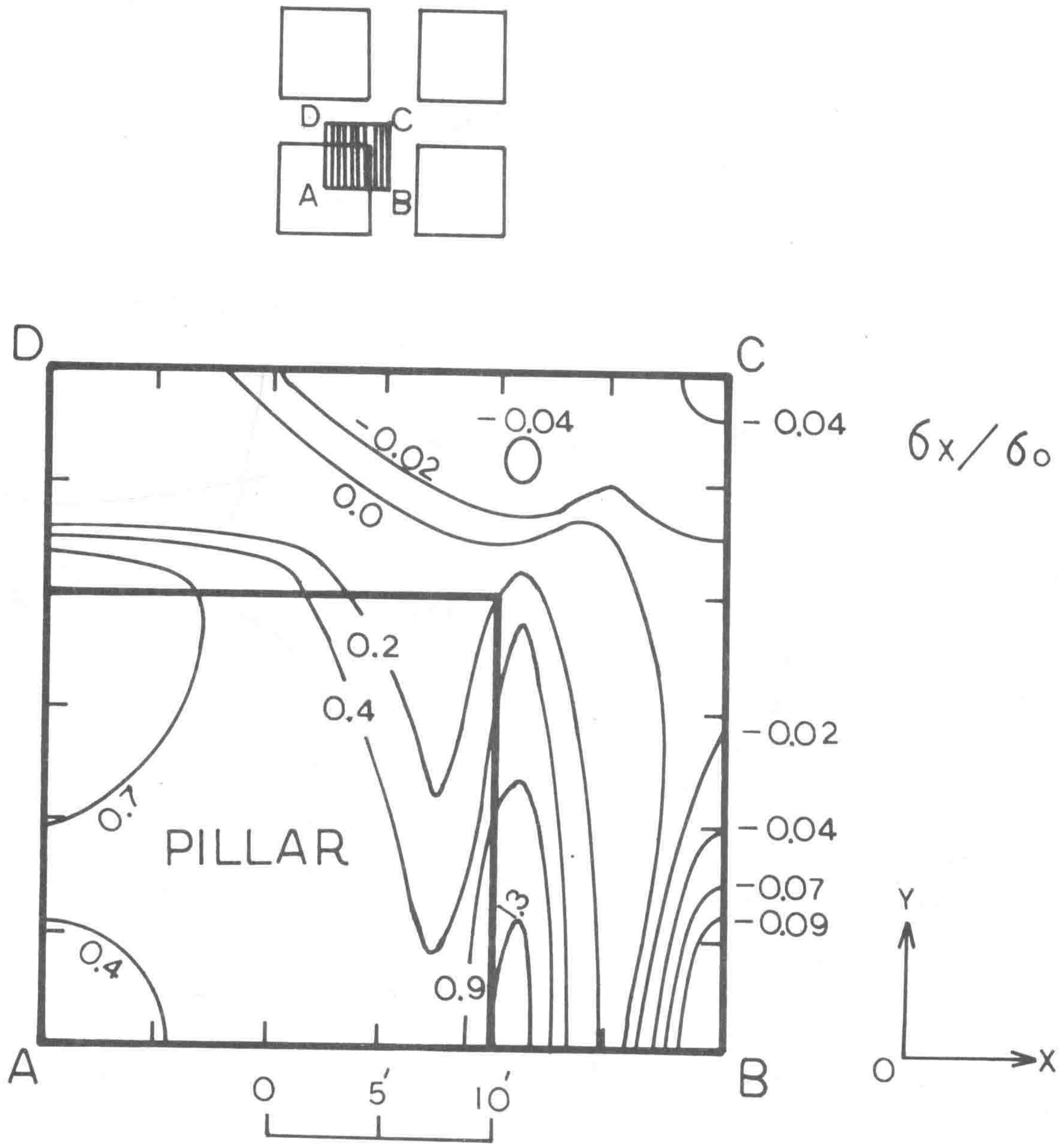

Fig. 11 Horizontal Stress Contour at 1 Ft. Above the Roof Plane - 20 Ft. Entry Intersection

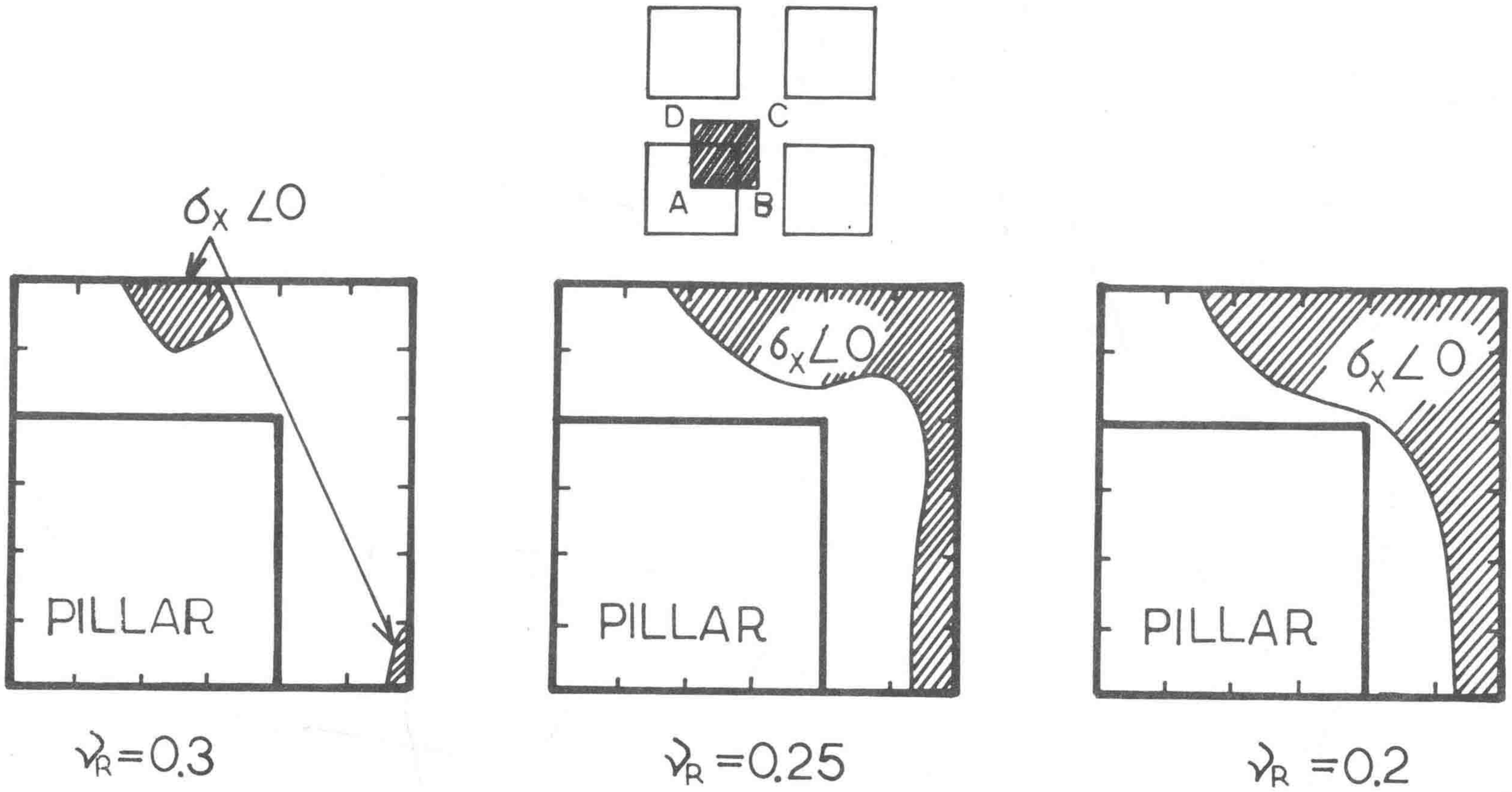

Fig. 12 Horizontal Stress Contour Line of $\sigma_x = 0$ at 1 Ft. Above the Roof Plane for Various Values of the Poisson's Ratio of Rock - 20 Ft. Entry Intersection

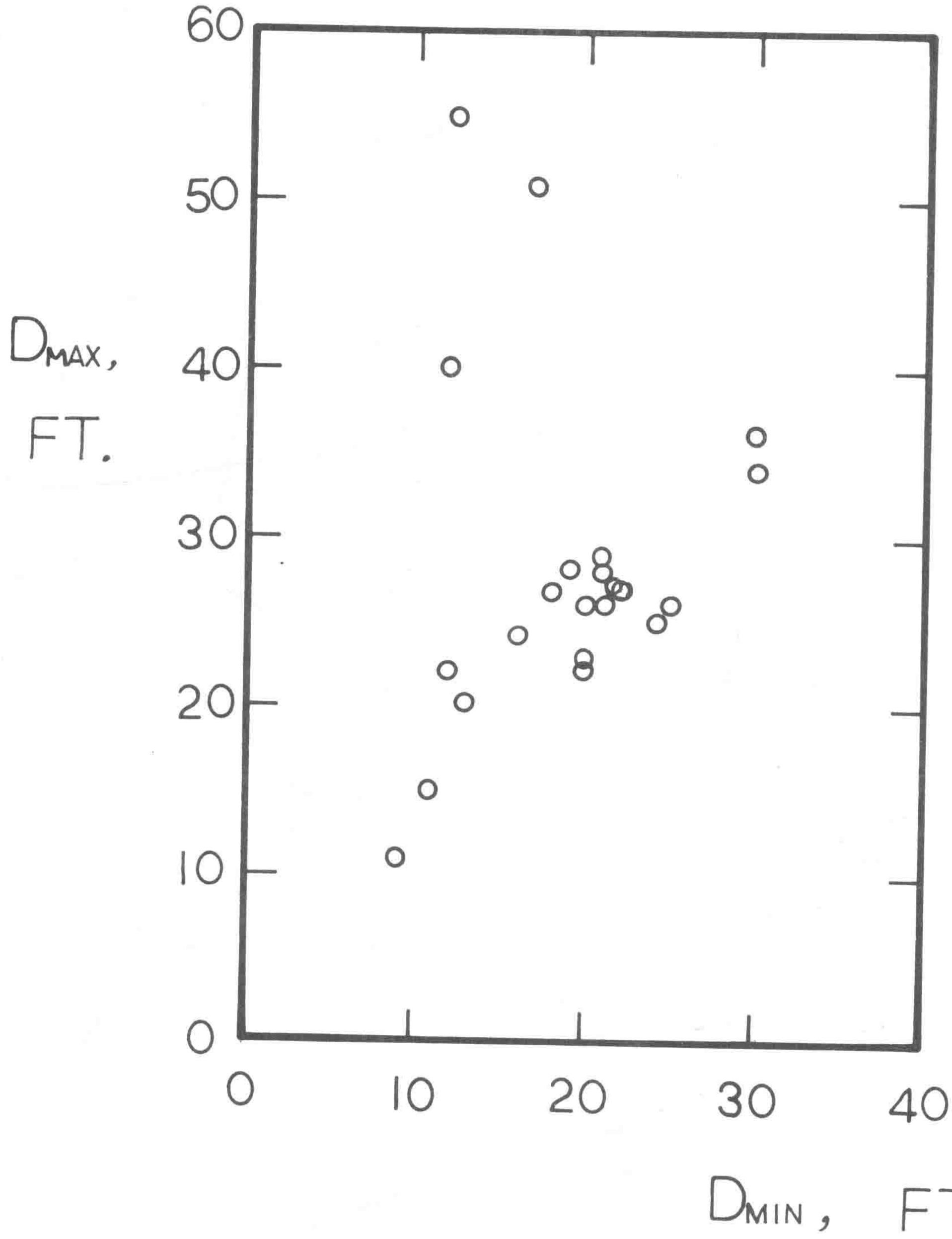

Fig. 13 Maximum and Minimum Diameters of Roof Falls at the 4-Way Entry Intersections

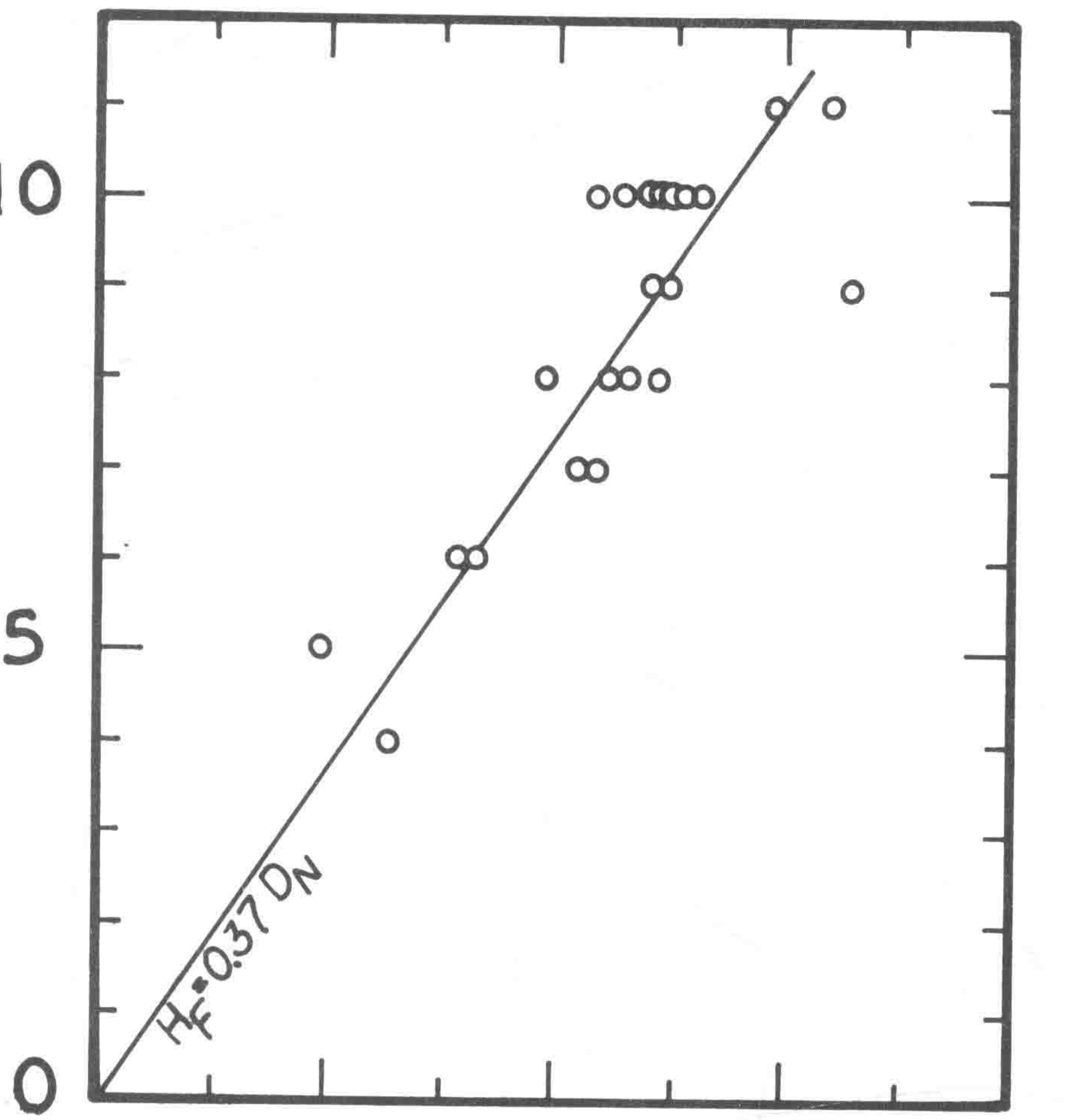

Fig. 14 Average Height of Roof Falls at the 4-Way Entry Intersections

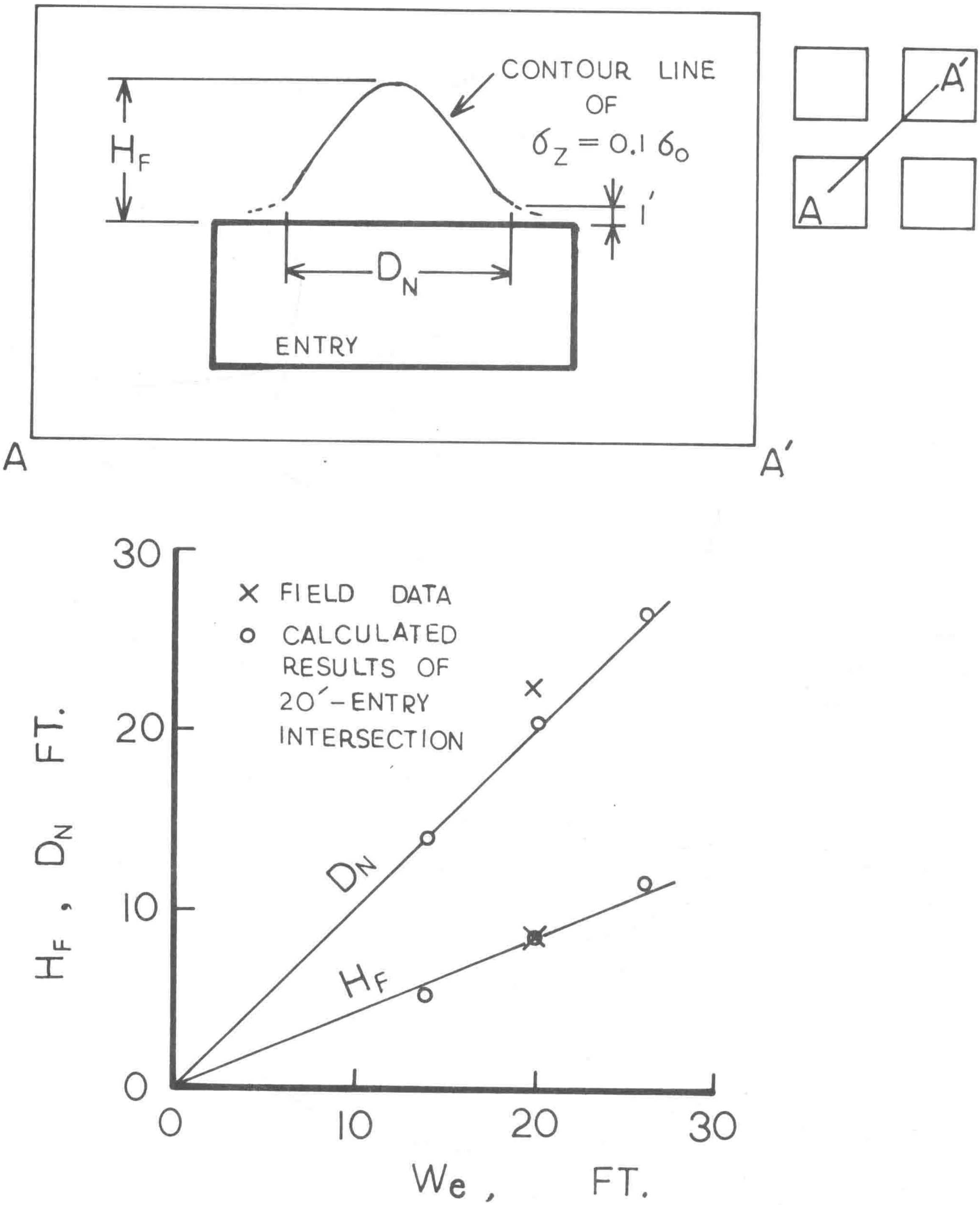

Fig. 15 Computed Arching Zones Vs. the Average Fall Shape

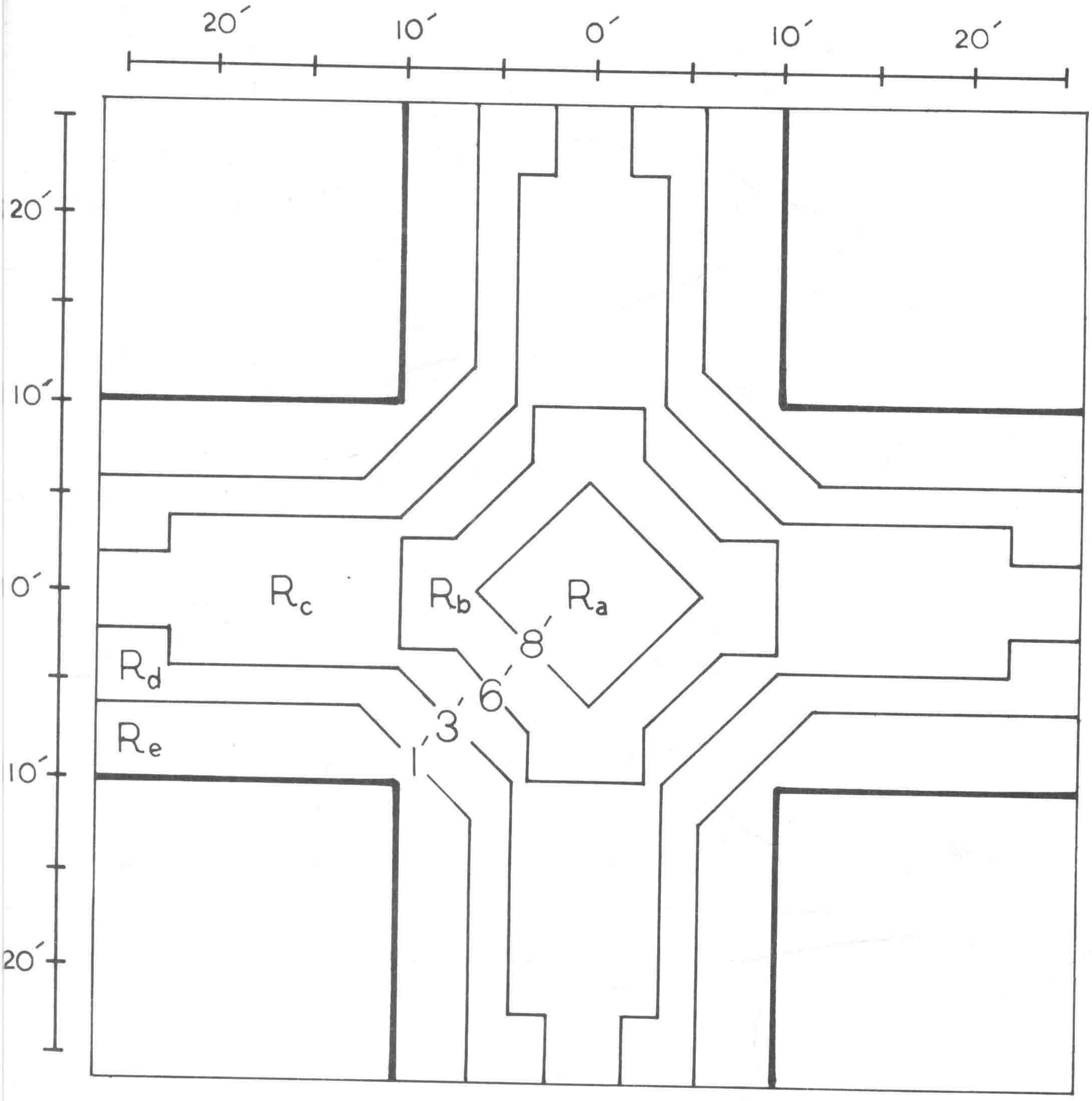

	HEIGHT TO THE APCHING ZONE (ft)
R_a	8 — 9
R_b	6 — 8
R_c	3 — 6
R_d	0 — 3
R_e	LESS THAN 1

Fig. 16 The Preferable Bolting Patterns for the 4-Way Entry Intersections-20 Ft. Entry Intersection

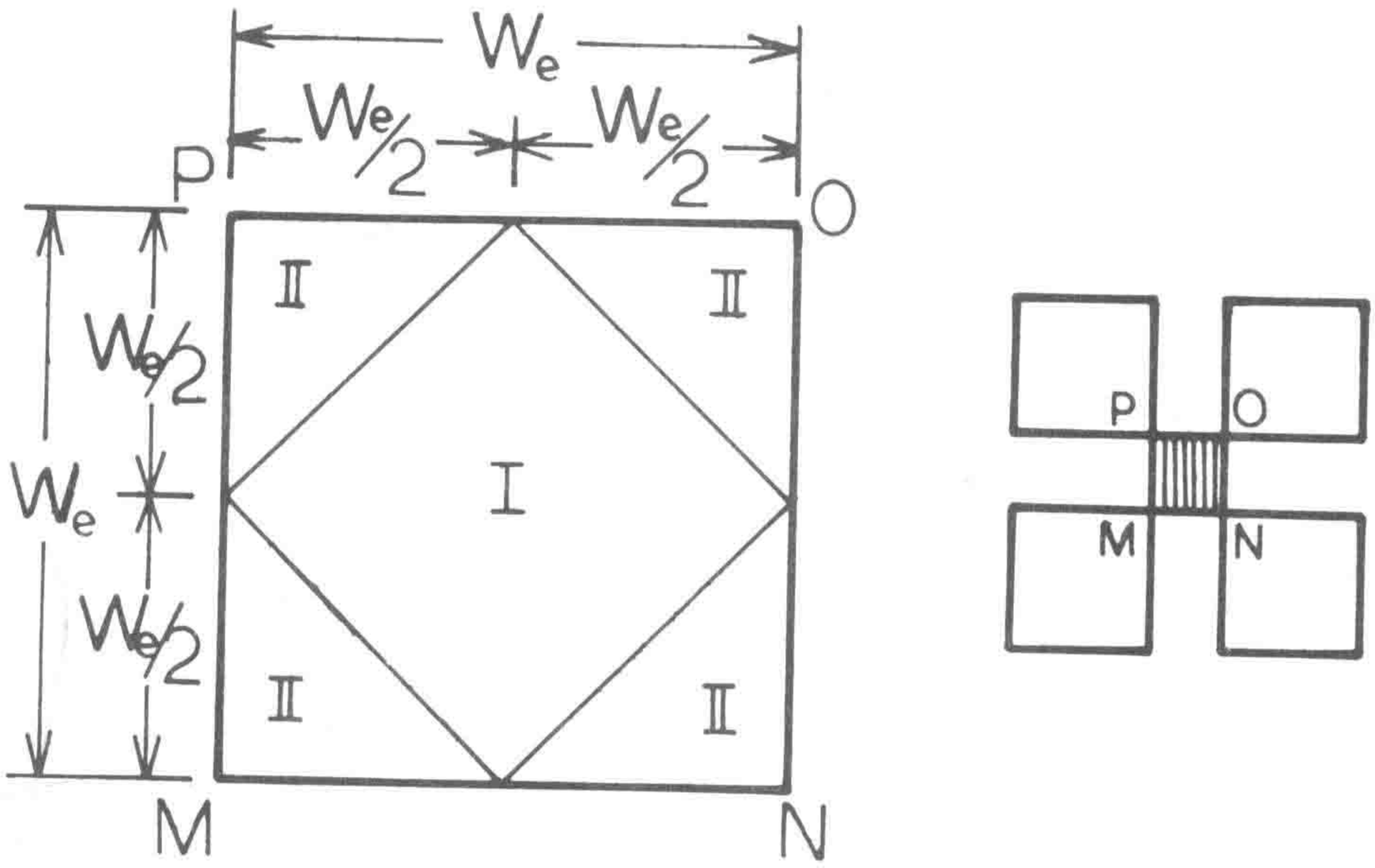

SUSPENSION METHOD	BOLT LENGTH	CARRING CAPACITY
REGION I	$\frac{1}{2} W_e$	$\frac{1}{2} \rho_R g W_e$
REGION II	$\frac{1}{4} W_e$	$\frac{1}{4} \rho_R g W_e$

REINFORCEMENT METHOD	BOLT LENGTH	REQUIRED SHEAR RESISTANCE	REQUIRED PRETENSION
REGION I	l_b	S_r	S_r / μ
REGION II	$0.8 \cdot l_b$	$0.4 \cdot S_r$	$0.4 \cdot S_r / \mu$

Fig. 17 The Proposed Bolting Patterns for the 4-Way Entry Intersections

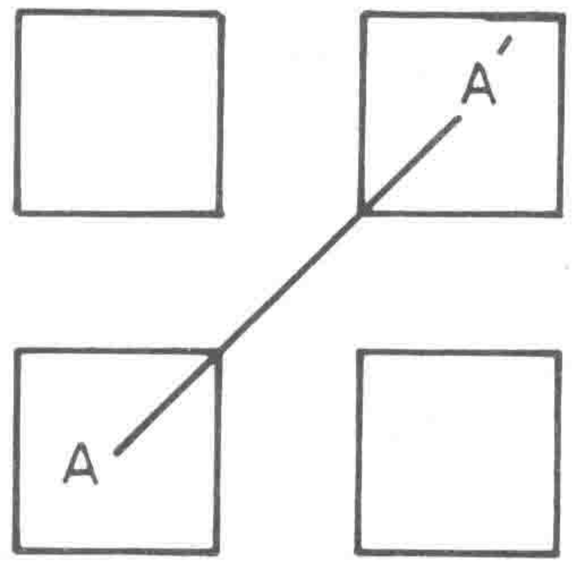

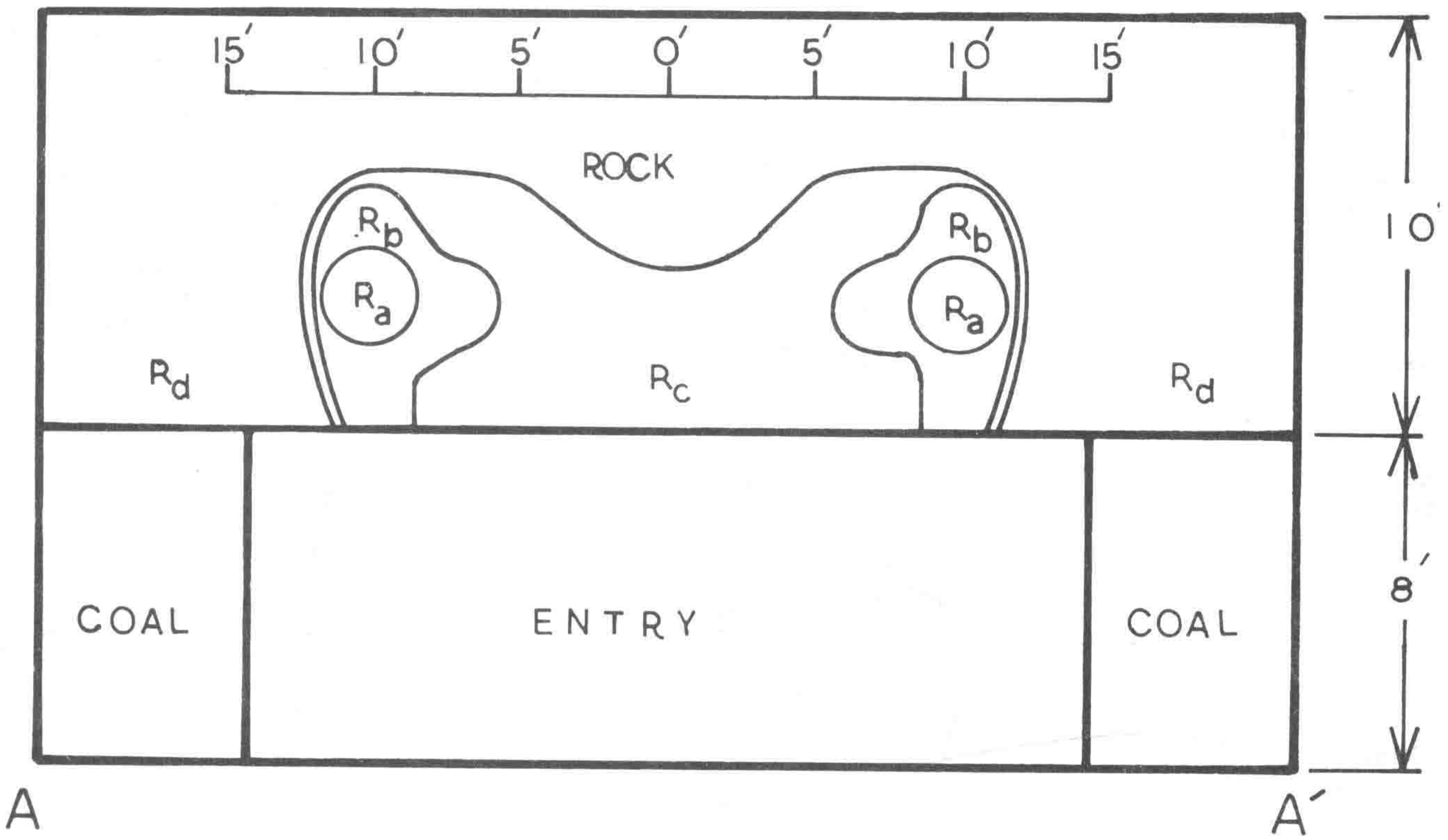

	S_r kip/ft²	S_r / σ_o
R_a	4 — 5	0.045 — 0.056
R_b	2 — 4	0.022 — 0.045
R_c	0 — 2	0 — 0.022
R_d	STABLE	STABLE

Fig. 18 Shear Resistances Required to Prevent Sliding at the Cross-Section AA' - 20 Ft. Entry Intersection

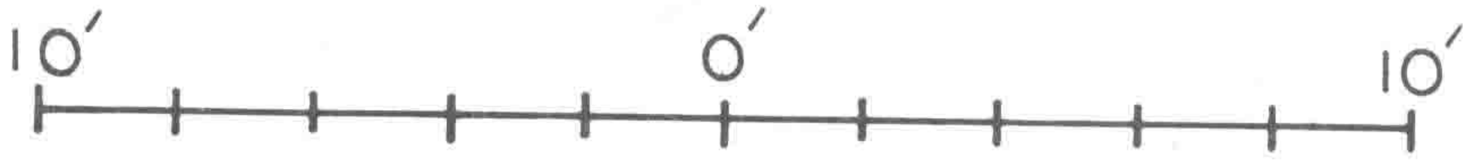

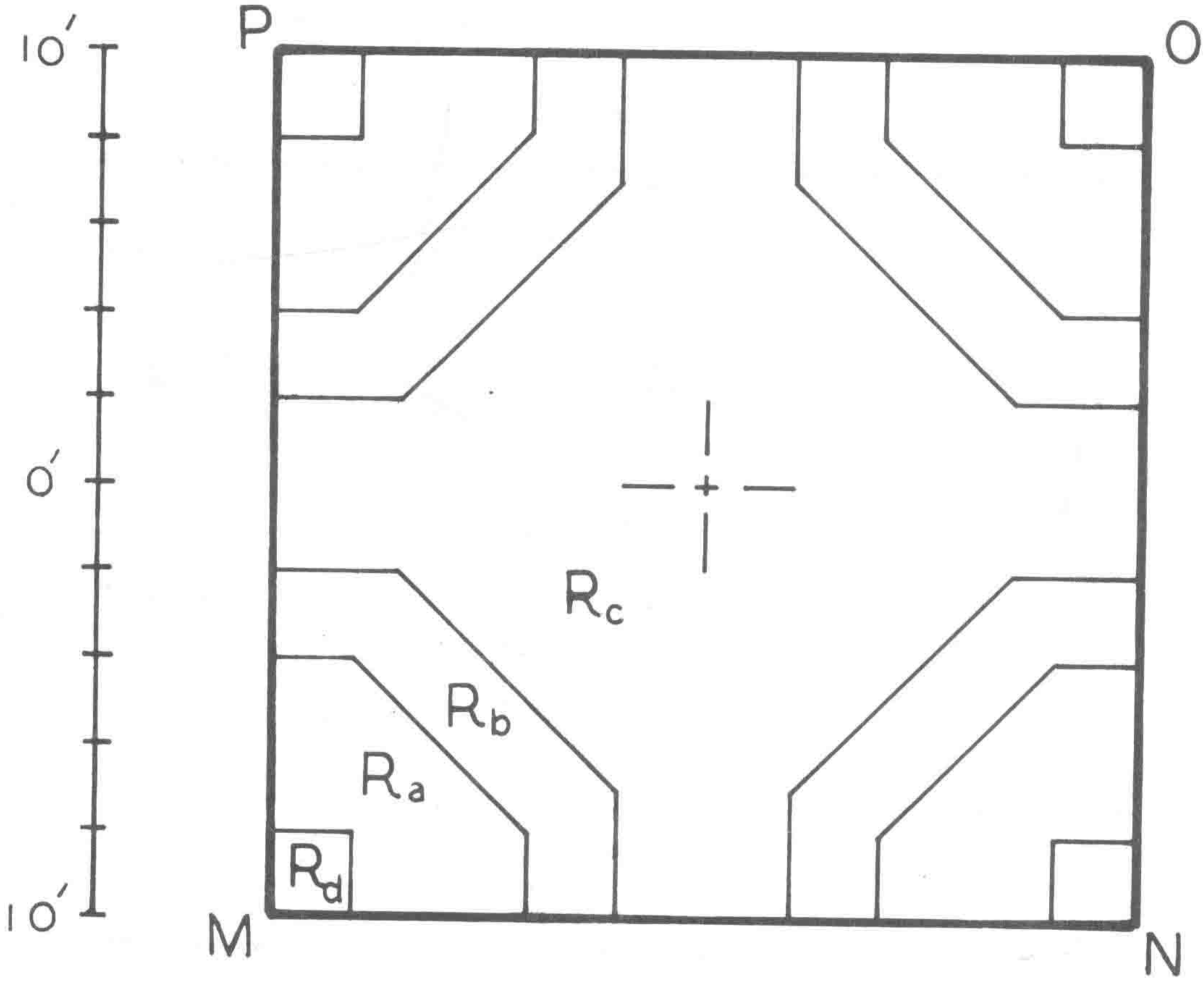

	S_r kip/ft²	S_r / σ_o
R_a	4 – 5	0.045 – 0.056
R_b	2 – 4	0.022 – 0.045
R_c	0 – 2	0 – 0.022
Rd	STABLE	STABLE

Fig. 19 Shear Resistances Required to Prevent Sliding at 3 Ft. Above the Roof Plane - 20 Ft. Entry Intersection

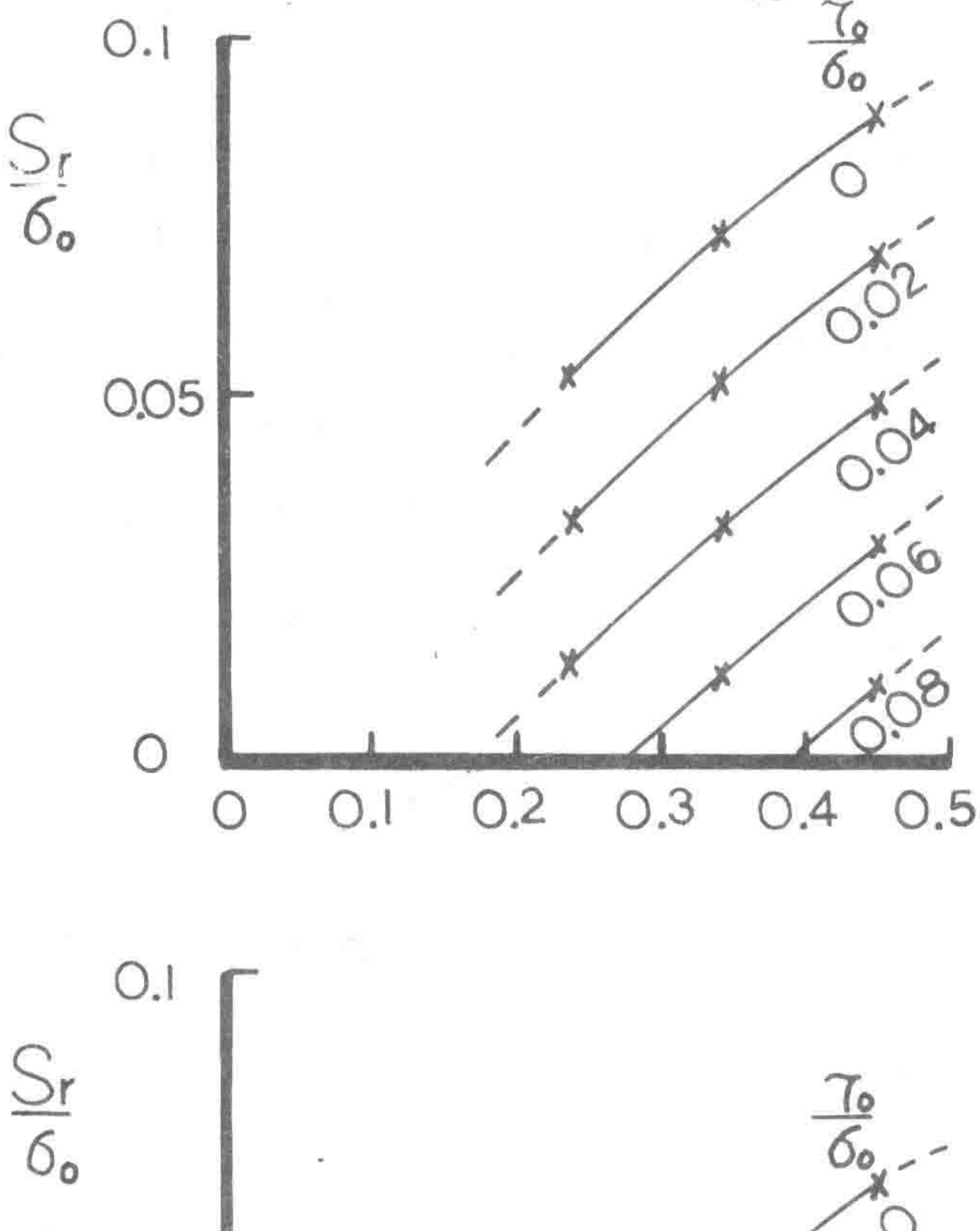

(a)

$\mu = 0.8$

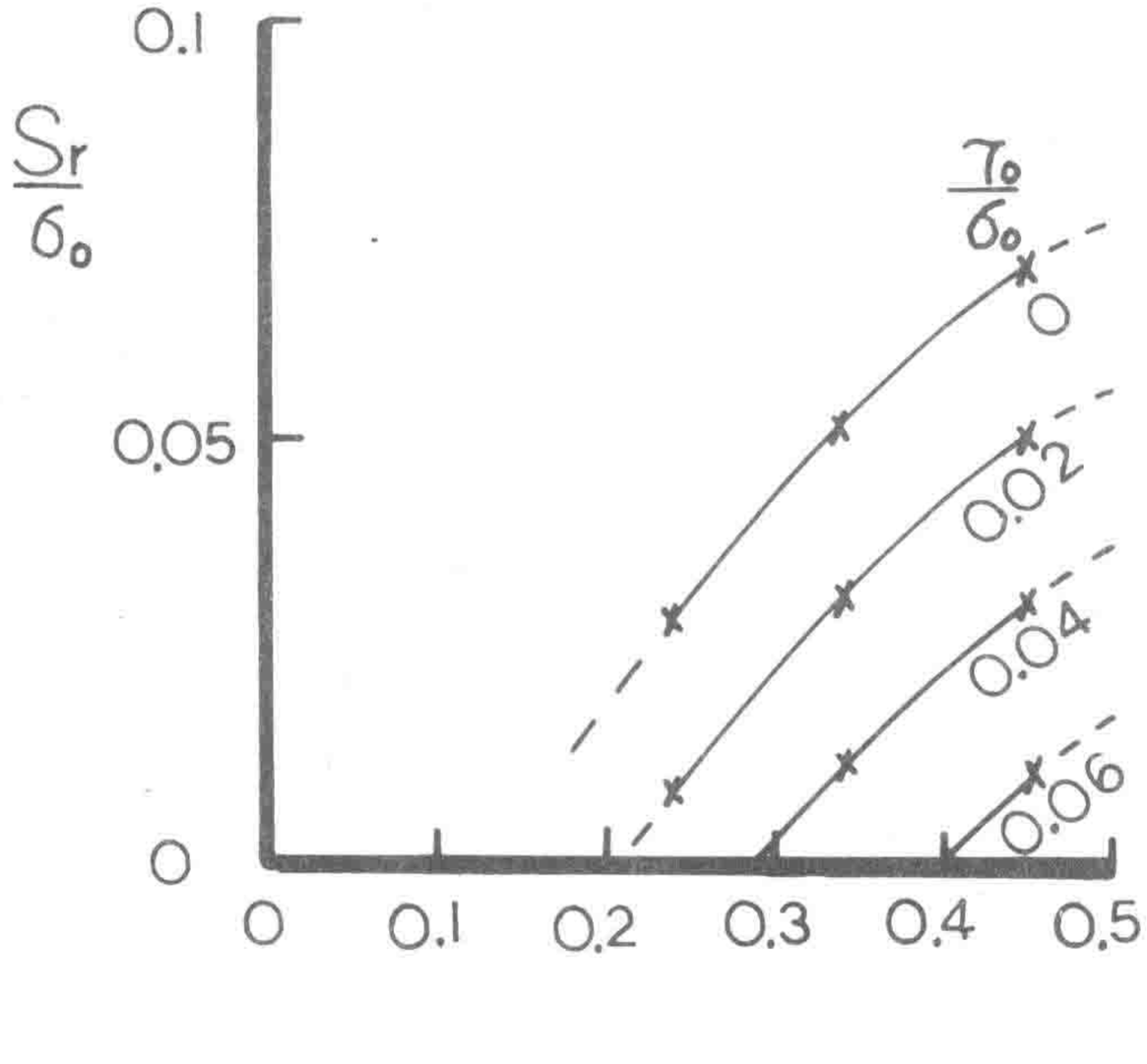

(b)

$\mu = 1$

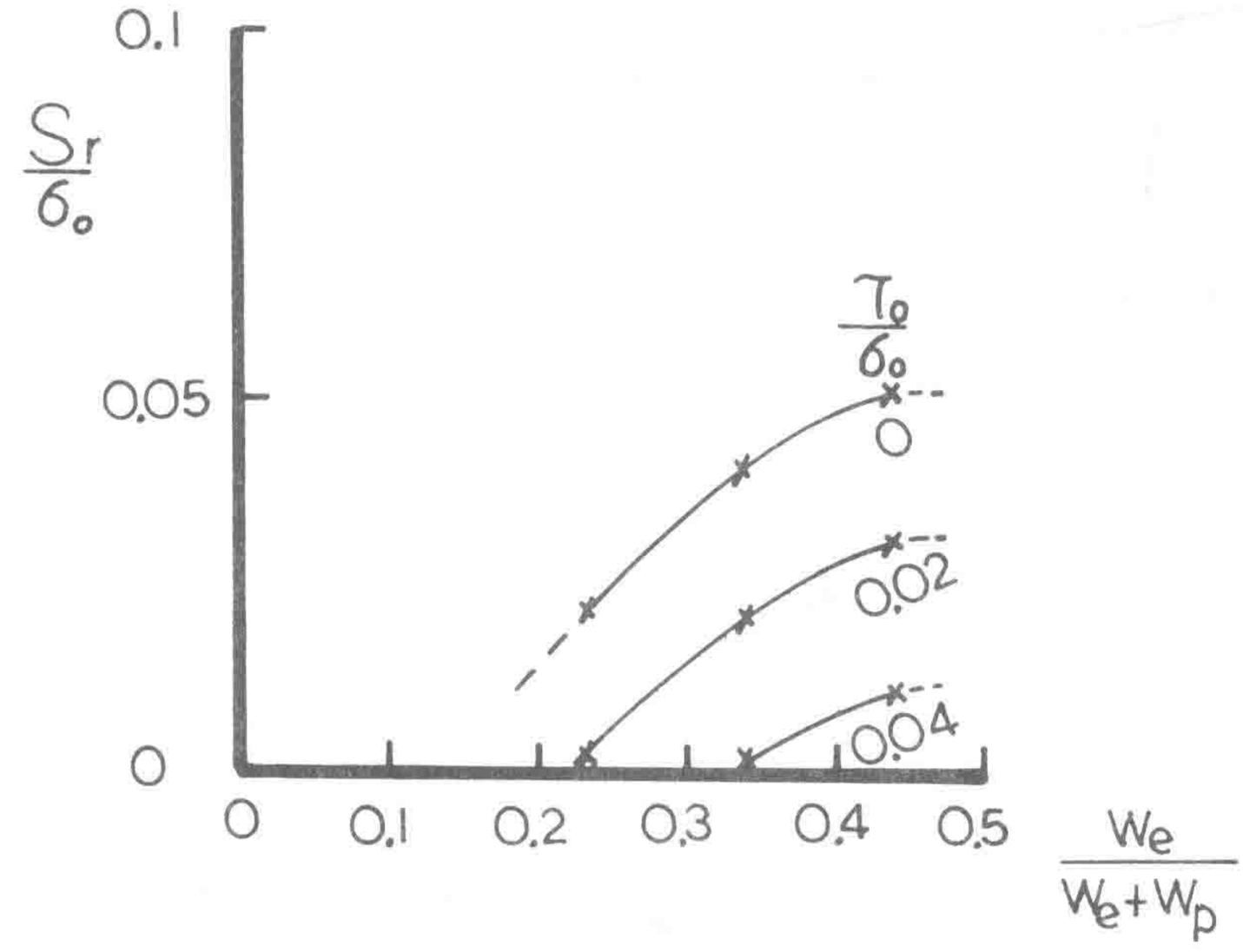

(c)

$\mu = 1.2$

Fig. 20 Shear Resistance Required for Various Combinations of μ, $W_e/(W_e+W_p)$, and τ/σ_c

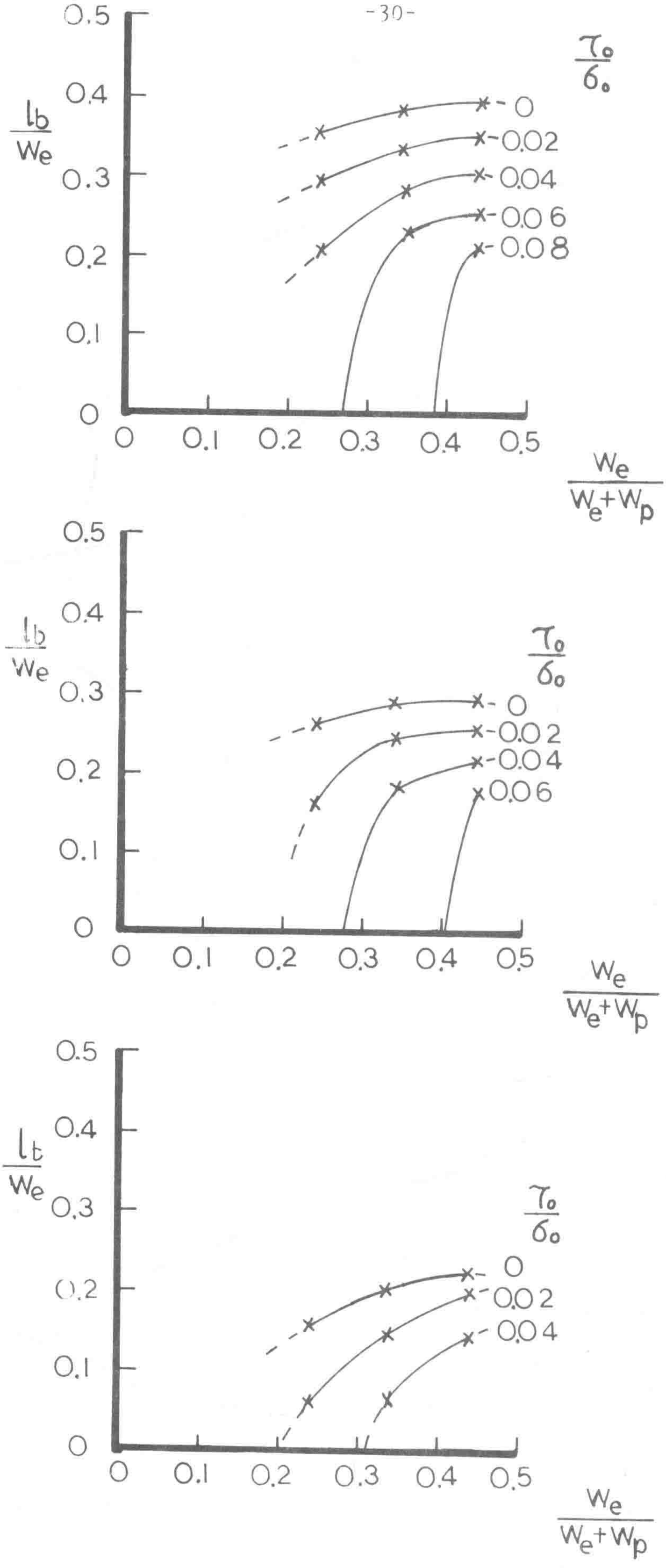

Fig. 21 Bolt Lengths Required for Various Combinations of μ, $W_e/(W_e+W_p)$, and τ_o/σ_o